Agricultural and Forest Meteorology 316 (2022) 108849

Contents lists available at ScienceDirect

Agricultural and Forest Meteorology

journal homepage: www.elsevier.com/locate/agrformet

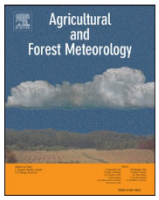

Recent trends in the agrometeorological climate variables over Scandinavia

Abhay Devasthale [a,*], Thomas Carlund [b], Karl-Göran Karlsson [a]

[a] Research and Development Department, Swedish Meteorological and Hydrological Institute (SMHI), Folkborgsvägen 17, Norrköping 60176, Sweden
[b] Information and Statistics Department, Swedish Meteorological and Hydrological Institute (SMHI), Folkborgsvägen 17, Norrköping 60176, Sweden

ARTICLE INFO

Keywords:
Agrometeorology
Climate change
Remote sensing
Precipitation
Clouds
Radiation

ABSTRACT

The impacts of global climate change in response to increasing greenhouse gasses are spatio-temporally heterogeneous and are observed in a number of essential climate variables (ECVs). Among the ECVs that are highly relevant for the agriculture and forestry applications are clouds, precipitation and the incoming surface solar radiation (SIS). The past trends in these three agrometeorological ECVs and, more importantly, the co-variability among them can impact future agriculture and forestry policies and practices, their resilience and conservation. Therefore, using 37-year long climate data records spanning from 1982 to 2018 from the satellite- and surface based observing systems, we investigate the co-variability of trends in cloudiness, precipitation and SIS over Scandinavia during the summer months (April through September).

The results reveal a complex nature of such co-variability among the trends in these three climate variables over Scandinavia. We report that the total cloudiness has decreased over much of Scandinavia. The decrease is most pronounced and statistically significant over southern Scandinavia in April, over the western coast in July and over much of northern Scandinavia in August. These decreasing trends are mainly due to reductions in the low and middle level clouds. The trends in all-sky incoming surface radiation are opposite in nature and broadly follow the spatio-temporal patterns of the trends in total cloudiness. The precipitation trends are heterogeneous, both spatially and temporally. The analysis of co-variability of trends reveals three distinct area-regimes that are relevant for assessing the changes in the land use and land cover.

1. Introduction

Incoming solar radiation at the surface, precipitation and cloudiness are among some of the most important essential climate variables (ECVs) relevant for agriculture and forestry. From the climate perspective, changes in their amounts and spatial distribution have a huge impact not only on the future agriculture and forestry policies and practices (Skogsstyrelsen, 2019), their resilience and adaptation (Keskitalo et al., 2016; Ambros and Granvik, 2020), but also on the sustainable use of the natural resources and the conservation practices (Skogsstyrelsen, 2019; Grusson et al., 2021b). These three ECVs not only have a direct impact on the growth of biomass and crop yield at shorter time scales, but they also interact and indirectly affect other variables essential for agriculture and forestry management such as surface temperatures, soil moisture, evapotranspiration etc (Guenni et al., 1990; Chmielewski and Rötzer, 2001; Lagergren and Lindroth, 2002; Kanniah et al., 2013; Watson and Challinor, 2013; Devasthale and Norin, 2014; Schurgers et al., 2015; Jönsson and Lagergren, 2017; Sikma et al., 2018; Jin et al., 2019).

The co-variability among these three ECVs is also relevant to study in the agrometeorological context. For example, although clouds are directly responsible for precipitation, not all clouds are the source of precipitation. Increased cloudiness doesn't necessarily increase water availability for the agricultural use. Clouds regulate incoming solar radiation. The more the cloudiness, the lesser the radiation available for the photosynthesis. However, the reality is often more complex. For example, while the optically thicker clouds could block the solar radiation and tend to reduce the agricultural and forestry yields, the thinner or broken clouds could lead to more multiple scattering of radiation and thus more diffuse radiation that could favor the growth of certain plants. Therefore, understanding the simultaneous changes in these three ECVs would provide a more complete picture of such interactions (Young and Smith, 1983; Gu et al., 1999; Still et al., 2009; Kanniah et al., 2013; Cheng et al., 2016; Proctor, 2021).

The satellite-based datasets show a greening of our planet in response to increased carbon dioxide emissions (Zhu et al., 2016). It is

* Corresponding author.
E-mail address: abhay.devasthale@smhi.se (A. Devasthale).

https://doi.org/10.1016/j.agrformet.2022.108849
Received 31 March 2021; Received in revised form 26 January 2022; Accepted 27 January 2022
Available online 3 February 2022

however recently reported that this climate-scale CO_2 fertilization may have reached its limit (Wang et al., 2020). This implies that the changes in agrometeorological or biometeorological variables would have a larger bearing on greening in future, especially at the shorter time scales. Both global and regional climate models provide a consensus that the climate change will benefit the agricultural and forestry practices in future in the European high latitude countries such as Sweden, mainly via increased temperatures and precipitation (IPCC, 2014; Rutgersson et al., 2015; Kjellström et al., 2018; Jia et al., 2019). It is however difficult to forecast how the complex interactions among these three ECVs would evolve in future and, more importantly, which regional effects the changes in their properties would have in future. In this context, the lessons could be learned from investigating the historical datasets, not only to understand how the state of the climate relevant for agrometeorology has been in the past, but also to evaluate if the climate models can indeed simulate the complex co-variability of the agrometeorological variables.

In light of this, the present study investigates the trends in the three ECVs mentioned above, i.e. all-sky surface incoming solar radiation (SIS), precipitation and cloudiness, over Scandinavia with particular focus on Sweden during the last nearly four decades. We use a combination of the state-of-the-art satellite-based climate data records of cloud properties and SIS together with ground-based data records of precipitation as well as SIS. We specifically aim to address the following scientific questions.

- Are clouds changing over Scandinavia? Which regions and seasons are sensitive to the changes in cloudiness?
- How are precipitation and SIS changing in relation to the changes in cloudiness over those sensitive areas?
- Do the satellite-based and ground-based records of SIS agree with one another?

The present study is novel in two aspects. (1) For the first time, we investigate multi-decadal trends in cloudiness and incoming solar radiation over the study area. Having this information on the regional trends is critical for the agrometeorological applications at a climate scale. Also unique is the use of satellite observations for this purpose. We also investigate trends in precipitation. (2) We provide, also for the first time, the regime driven maps that show the interplay of trends among these variables. These maps will not only be valuable for the process oriented investigations of climate models that have dynamic vegetation component over the study area, but they also visually highlight regions that are sensitive to changes relevant for the agricultural activities.

2. Data and methods

We use the climate data records of cloud properties and SIS from CLARA-A2 and CLARA-A2.1 (Karlsson et al., 2017; https://doi.org/10.5676/EUM_SAF_CM/CLARA_AVHRR/V002_01). This second edition of the EUMETSAT's Satellite Application Facility on Climate Monitoring (CM-SAF) cloud and radiation data record extends from 1982 to 2018 and is based on a series of Advanced Very High Resolution Radiometer (AVHRR) sensors flown on the National Oceanic and Atmospheric Administration (NOAA) and EUMETSAT's MetOp satellites. CLARA-A2 has a rich history of continuous development in the framework of CM-SAF (https://www.cmsaf.eu/) since 1998 and has matured considerably to climate quality in the last decades (Karlsson, 2003; Dybbroe et al., 2005; Karlsson et al., 2013; Karlsson et al., 2017; Karlsson and Devasthale, 2018). It has been rigorously studied and evaluated globally, especially over the northern European domains, which is highly relevant for the present study. The detailed documentation on the cloud property and SIS retrieval algorithms, including their evaluations and comparisons with other observations can be found in Karlsson and Dybbroe (2010), Karlsson et al. (2017), Riihelä et al. (2015), and Pfeifroth et al. (2018).

The original footprint of the Global Area Coverage (GAC) data from the AVHRR sensors is about 5 km. The cloud property retrievals are performed at this original resolution and then gridded at 0.25 deg regular grid and the daily means are computed (referred to as Level 2 data). This daily information is then used to compute the Level 3 monthly means. Here, we used these Level 3 monthly mean products that are also available at 0.25 by 0.25° regular grid from January 1982 to December 2018 covering the entire 37-year period. These products are suitable for climate studies and investigating the climate variability and trends. The CLARA-A2 dataset provides information on cloud amount and cloud physical and microphysical properties such as cloud top temperature, pressure, height, cloud liquid/ice water path, optical depth, and liquid droplet/ice crystal effective radius. The dataset also provides the retrievals of SIS. Here, we have used cloud amount (also for low-, middle- and high-level clouds), cloud liquid water path and SIS.

Following the Internal Satellite Cloud Climatology Project (ISCCP) cloud typing conventions, we also investigated the trends in three main cloud types, i.e., low, middle and high level clouds separately. Low clouds represent clouds with cloud top pressures higher than 680 hPa and typically contain stratus, stratocumulus and shallow cumulus clouds. Middle levels clouds (CTP $>$ 440 hPa) represent mainly altocumulus and stratocumulus clouds over Scandinavia and high level clouds (CTP $<$ 440 hPa) represent mainly cirrus and cirrostratus clouds. It is to be noted that, due to cloud type missclassifications depending on the quality of reanalysis data that is used as one of the ancillary inputs in the cloud property retrieval algorithm, some of low level clouds can end up in the middle level category. However, the low- and middle-level clouds when considered together should represent the vast majority of clouds that are responsible for liquid precipitation.

We further use the data from the Global Precipitation Climatology Center (GPCC) that provides quality-controlled reanalysis of precipitation based on the global network of ground-based measurement stations (Becker et al., 2013; Schneider et al., 2014). The data from the Scandinavian measurement stations operated by the respective national weather services including SMHI are integrated into this reanalysis. We specifically use the Full Data Monthly Product Version 2020 (obtained from https://www.dwd.de/EN/ourservices/gpcc/gpcc.html) at the 0.25 by 0.25° grid for the 1982–2018 period, same as in the case of CLARA-A2.

This GPCC dataset does not rely on satellite estimates and therefore provides an objective, independent estimate of precipitation that is not influenced by clouds as usually is the case for the satellite sensor derived estimates of precipitation.

In addition, we use the ground-based measurements of SIS available at the 17 surface stations. In Sweden, fully automated solar radiation observations have been operated by SMHI since 1983. The first automated network ran more or less unchanged until 2007. A network upgrade was carried out during 2006–2007 and the updated stations became operational from 2008. In 2007 the old and new stations were operated in parallel. The stations which have been used in this study are both the twelve long-term stations which have been and still are in operation since 1983 (Borlänge since 1987) as well as five newer stations with start dates 2007 or later. These are listed in Table 1 and their locations are also shown in Fig. 6.

The Swedish measurements, both before and after 2008, are described in more detail by Carlund (2011). In that report also results of the comparison of the old and new measurements are presented. Over the whole comparison period of about a year the ratio of accumulated global irradiation from the old versus the new network was 0.997. The value of 1.0 would indicate the newer and older networks ideally measure exactly the same amount of radiation. Monthly global irradiation values at individual stations differed normally 1% or less during the summer half year. During November-January, the monthly values could differ 5%, or even more, mostly with the old measurements being higher than the new ones.

SMHI pyranometer calibrations are performed outdoors at the main

Table 1
Locations of the SMHI SIS measurement stations used in this study. The spatial locations of these stations are shown in Fig. 5.

ID	Station	Latitude °N	Longitude °E	Altitude m	Start year
1	Tarfala	67.911	18.607	1144	2007
2	Kiruna	67.842	20.410	424	1983
3	Luleå	65.544	22.111	32	1983
4	Umeå	63.811	20.240	23	1983
5	Storlien-Visjövalen	63.302	12.124	646	2013
6	Östersund	63.197	14.480	374	1983
7	Borlänge	60.488	15.430	164	1987
8	Svenska Högarna	59.442	19.502	10	2007
9	Karlstad	59.359	13.472	46	1983
10	Stockholm	59.353	18.063	30	1983
11	Nordkoster	58.892	11.004	33	2010
12	Norrköping	58.582	16.148	43	1983
13	Göteborg	57.688	11.980	30	1983
14	Visby	57.673	18.345	49	1983
15	Växjö	56.927	14.731	182	1983
16	Hoburg	56.921	18.151	34	2013
17	Lund	55.714	13.212	90	1983

station in Norrköping. The field instruments are compared to field reference instruments, which are calibrated against SMHI's secondary standard pyrheliometers, which in turn are calibrated at the International Pyrheliometer Comparisons held every fifth year at the Physikalisch-Meteorologisches Observatorium Davos/World Radiation Center in Davos, Switzerland. In 2012, a reginal pyranometer comparison was held in Norrköping, showing that most participating instruments agreed within 1% for time integrated global radition over a week (Carlund, 2013).

These surface measurements are used to evaluate the CLARA-A2 estimates of SIS over Sweden and also to perform a complementary trend analysis.

We analyze climatological features and trends in these datasets for each month separately. Since the focus is on agrometeorology, we investigate all datasets for the summer half year from April to September. In the case of cloudiness, precipitation and SIS datasets, at each 0.25 × 0.25 deg grid, we used a simple linear regression to compute the trends over the 37 monthly means (for each summer month). The statistical significance is tested using the Mann-Kendall test (Mann, 1945; Kendall, 1975) and only those trends that are significant at 95%ile are shown.

While doing comparisons with the SIS data at the Swedish measurement stations, we chose the CLARA-A2 gridpoint that is geographically nearest to the station location. The mean bias, root mean squared bias and Pearson's correlation coefficient are calculated as follows.

$$Mean\ Bias = \frac{1}{n}\sum_{1}^{n}(C-S) \tag{1}$$

$$Root\ Mean\ Square\ Bias = \sqrt{\frac{1}{n}\sum_{1}^{n}(C-S)^2} \tag{2}$$

$$Pearson's\ correlation\ coefficient = \frac{\sum_{i=1}^{n}(C-C_m)(S-S_m)}{\sqrt{\sum_{i=1}^{n}(C-C_m)^2}\sqrt{\sum_{i=1}^{n}(S-S_m)^2}} \tag{3}$$

Where, n is the number of samples (37 in this case), C and S are the CLARA-A2 and the measurement station incoming solar radiation data, respectively, and Cm and Sm are the respective climatological means.

3. Results and discussions

The results are presented as follows. A climatological overview of cloudiness, precipitation and SIS is first presented for each month from April to September, followed by the discussion of trends therein. The comparisons and evaluations of CLARA-A2 SIS with the surface measurements is presented in the next subsection and finally the regime analysis providing the synthesis of trends in shown in the final subsection.

3.1. Climatological overview and co-variability

All three climate variables investigated here, i.e. cloudiness, precipitation and SIS, have a discernible intraseasonal variability during the summer half year over Scandinavia. This intraseasonality can be seen in Fig. 1 that shows their climatological mean values for each month from April to September, averaged over the entire 37-year study period (i.e. 1982–2018). While the cloudiness remains high between 80–95% over the Norwegian Sea throughout summer, the Baltic Sea, on the other hand, has a distinct intraseasonality, with lowest cloudiness observed in May. The Scandinavian mountain range also shows high cloudiness throughout summer, although the skies are slightly clearer during August. The all-sky incoming surface radiation, modulated by clouds, follows a noticeable intraseasonality, peaking during June over Scandinavia as a whole. The uncertainties in the satellite sensor derived SIS retrievals in the Scandinavian mountains are high when there is still considerable snow blanketing these regions and therefore these regions are masked out during April and May. The cloudiness in September is higher than in April and the atmosphere is also more opaque due to higher water vapor, therefore the SIS is lower over the northern Scandinavia.

The strongest heterogeneity in the spatial distribution among all variables is however observed for the precipitation. Note that the GPCC reanalysis covers only the mainland regions and the neighboring islands (which is relevant in the agrometeorological context here) and therefore the data over the open seas are missing. The southwestern and western coasts of Scandinavia experience high precipitation and the lowest intraseasonality. These regions are strongly influenced by the dominant southwesterly and westerly winds that bring warm and moist airmasses from the Northeast Altantic and the continental Europe, precipitating heavily along the Scandinavian coasts (Devasthale and Norin, 2014; Norin et al., 2017). The central and southern Scandinavian inland areas show a clear peak in precipitation in July, followed very closely in August. The lowest precipitation is observed in April, especially in the northern Lapland region.

We further investigated the co-variability among these three agrometeorological variables in detail using the detrended time-series of two variables at a time at each grid point. The results are shown in Fig. 2. These results show that cloudiness and surface radiation are, as expected, negatively correlated. However, there are spatial variations in the correlation magnitudes. These variations are mainly driven by the occurrence of different types of clouds over the study region and their interaction with the radiation. For example, high thin clouds and lower broken clouds, depending on their optical thickness, would still permit some solar radiation to reach the surface leading to weaker correlations, while the optically thicker clouds would block the radiation completely leading to stronger negative correlations. Cloudiness and precipitation are positively correlated. This is also expected since the presence of clouds is necessary for precipitation. However, not all types of clouds precipitate and the meteorological conditions are not favorable for precipitation each time clouds are present. This introduces variability in the magnitude of correlations between clouds and precipitation. The correlations are weaker over northern parts since this disconnect between clouds and precipitation is larger over northern Sweden due to very different meteorological conditions (temperature, humidity and atmospheric dynamics) compared to southern Sweden. Cloud systems are generally optically thicker during summer over the southern Sweden due to the transport of heat and moisture from the southern latitudes. The precipitation processes are more efficient and therefore a better connection between clouds and precipitation is observed compared to the northern regions. The correlation between precipitation and radiation is more complex because it depends on the diurnal cycles of all three

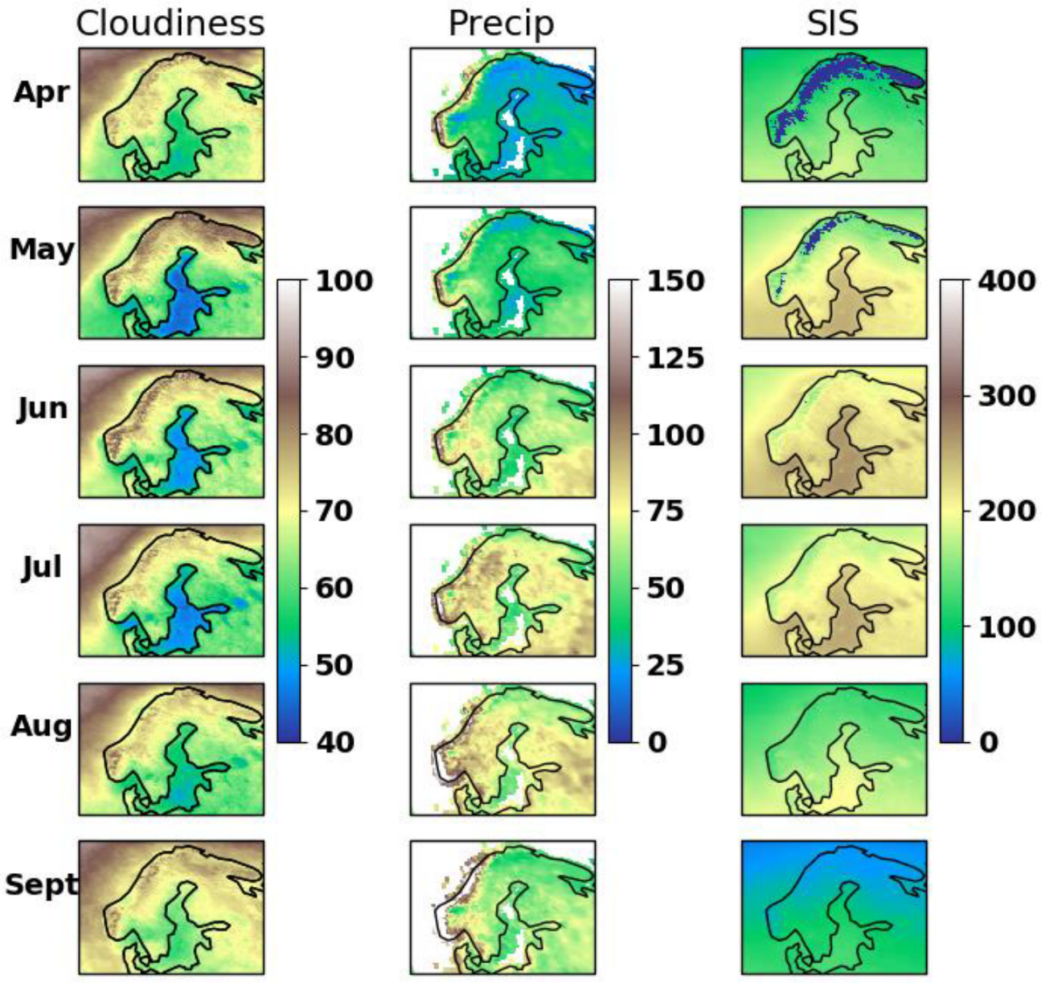

Fig. 1. Climatological distribution of total daytime cloud fraction (in %, left column), total precipitation (in mm, center) and SIS (in W/m^2, right column) based on 37-year data (1982–2018).

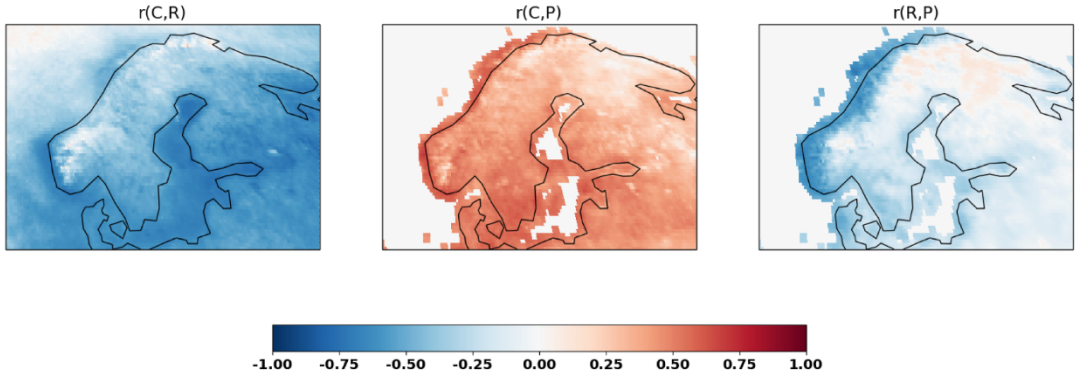

Fig. 2. Correlations between cloudiness (C), precipitation (P) and incoming solar radiation at the surface (R). All data from 1982 to 2018 and from April to September are used for the analysis.

variables. It may precipitate during the darker hours of the day when the incoming solar radiation is either absent or minimal. The stronger negative correlations between precipitation and radiation along the Scandinavian southern and westerns coasts are due to the presence of large-scale frontal systems that bring precipitation and persistent cloudiness as a result of warm and moist air mass transport from the westerly or southwesterly regions.

It is evident from the climatological overview presented in Figs. 1 and 2 that these three variables have a strong spatio-temporal heterogeneity and that their co-variability is non-linear. This is important to note not only in the agrometeorological context, but also to better interpret their climate trends in relation to one another.

3.2. Trends in cloudiness, precipitation and SIS

Fig. 3 shows the decadal trends in cloudiness, precipitation and SIS.

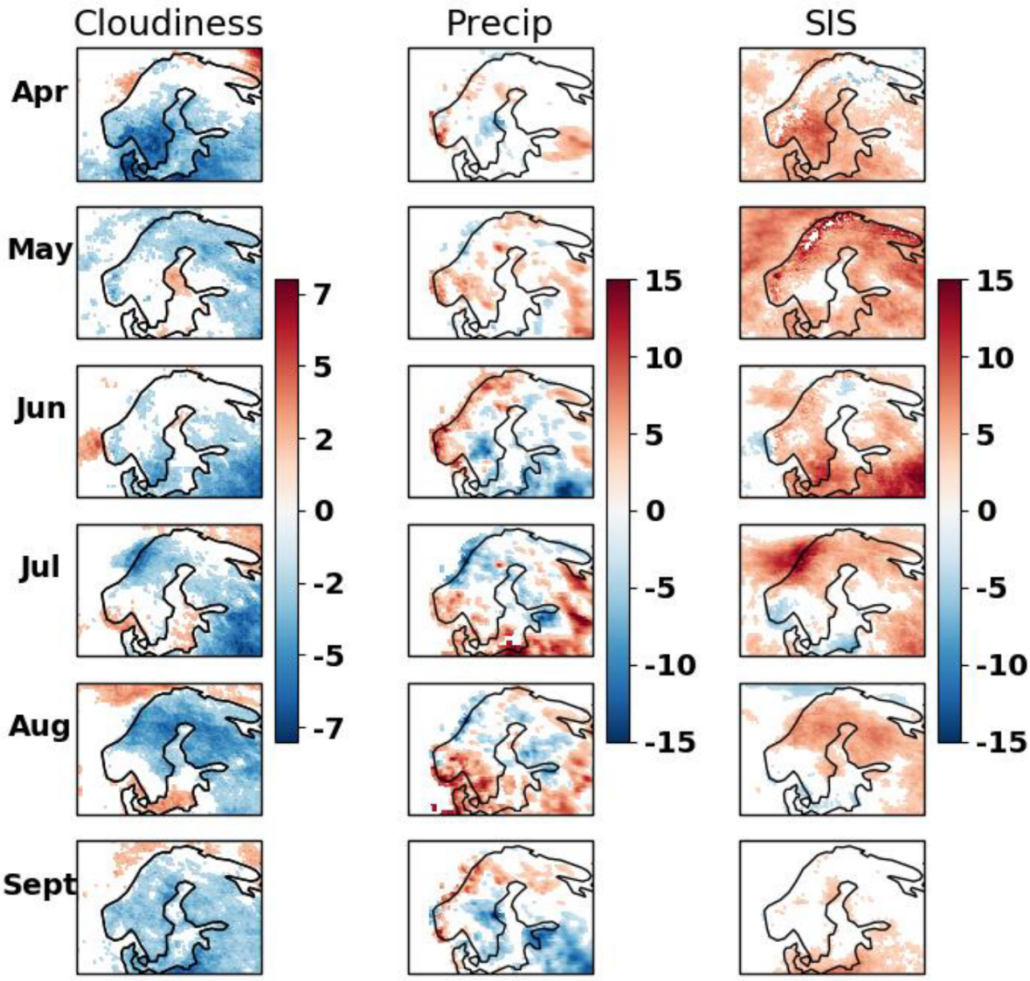

Fig. 3. Trends in total daytime cloud fraction (in %/decade, left), total precipitation (in mm/decade, center) and SIS (in W/m^2/decade, right). Only the trends that are statistically significant at 95% confidence are shown.

Cloudiness is decreased over the Scandinavian land areas in all summer months, although the magnitude and regionality of cloudiness decrease is very heterogenous. The trends in SIS broadly follow the opposite patterns, as the all-sky solar radiation reaching the surface is strongly regulated by clouds. In April, the southern parts of Scandinavia, especially the southern parts of Sweden, show a strong decreased cloudiness with trends reaching to 4–6% decrease per decade. As a result of these increased clear sky conditions, the SIS is increased at a rate of 5–7 W/m^2/decade over these regions in April. The cloudiness and SIS trends in the northern Scandinavia are not statistically significant in April. The cloudiness has also decreased over the nearby Baltic and North Sea areas.

In May, a somewhat opposite regionality in trends is seen. For example, the cloudiness shows no significant trends over Southern Sweden, instead there is a weaker but statistically significant increasing trend over the northern Lapland region, which co-varies with the SIS, in that, there is a corresponding increasing trend in SIS. In June, only the southeastern region of Sweden (parts of Skåne, Småland and Blekinge) show decreased cloudiness and a stronger increase in SIS. The north-central parts of Sweden and Norway and the central western coast of Norway show a pronounced decrease in cloudiness and increase in SIS during July. In fact, the increasing trend in SIS in July is strongest along central west Norwegian coast among all regions and months, with values upwards of 10 W/m^2/decade. While the majority of the Scandinavian land regions show a decreasing trend in cloudiness in August, the corresponding increases in SIS are weaker. There are no statistically significant trends in SIS over much of Scandinavia during August, although there is an overall weak decrease in cloudiness.

We further examined which cloud types contributed to the observed trends in total cloudiness and SIS. This is important to know since not all cloud types regulate the SIS and precipitation equally. It is evident from Fig. 4 that the overall decrease in total cloudiness was driven mainly by the decreases in low and middle level clouds over much of Scandinavia in the last four decades. The high level clouds in fact show the increasing trends, especially during the late summer months. The spatial variability in the trends of low, middle and high clouds is also interesting to note. For example, most of the inland areas and the western coastal areas that show strong decreasing trends in total cloudiness, also show strong decreasing trends in the middle level clouds. This is mainly because, these clouds are usually the result of either convective processes during warm summer months in the inland areas or the vigorous frontal systems that arrive and precipitate along the western coasts. Given that the surface temperatures have increased over Scandinavia in the last four decades in a warming world (Rutgersson et al., 2015; Krauskopf and Huth, 2020; Gulev et al., 2021) and that the atmospheric circulation regimes favor more transport of heat and moisture from the southerly latitudes, it is remarkable to note that the this has not translated into increases in low and middle level clouds. It is also worth pointing out the cloudiness decrease seen in the CLARA-A2 climate data record is consistent with all other space-based climate data records, suggesting the robustness of the trends (Karlsson and Devasthale, 2018). The corresponding increase in SIS is also consistent with the previous studies

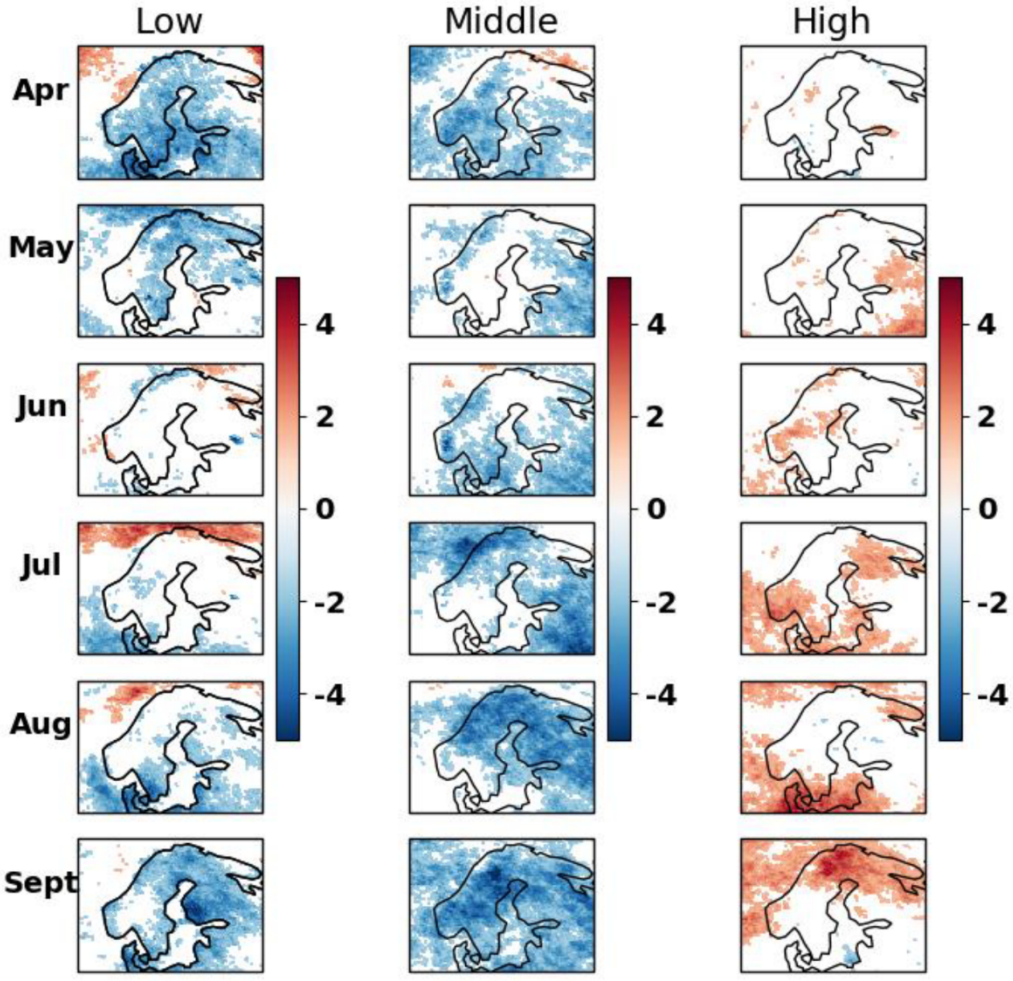

Fig. 4. Trends in low, middle and high cloud fraction (in %/decade). Only the trends that are statistically significant at 95% confidence are shown.

that include only southern parts of the study area and also use different datasets (Pfeifroth et al., 2018), further providing confidence in the analysis presented here.

While cloudiness and SIS are tightly connected, the co-variability between cloudiness and precipitation is highly non-linear, especially over the high latitude countries such as Scandinavians. This is mainly due to the fact that, unlike the tropical regions where radiative-convective processes primarily govern cloud and precipitation variability, the dynamical and baroclinic processes play a more important role in the high latitude regions. Non-precipitating boundary layer clouds topped by a temperature inversion are also typical for these regions. Furthermore, the presence of lee wave high cirrus clouds behind eastwards of Scandinavian mountain range is also a common feature. Therefore, a linear correspondence between clouds and precipitation is not always observed, even in the summer months. This is evident in Fig. 3 that shows that, unlike the homogeneous decreasing trends in total cloudiness, the precipitation trends are heterogeneous in nature, both spatially and temporally. For example, the precipitation has increased along the entire Norwegian coast during June, in spite of no statistical change in the total cloudiness. A similar feature can also be observed over southern Sweden during August and the north central parts during the September months. These regions do not show a statistically significant change in the total cloudiness during the respective months. This disconnect between trends in cloudiness and precipitation can be understood and explained by investigating the other cloud physical properties, such as cloud liquid water path, which provides important information on the water holding capacity of clouds. Most of the clouds during summer contain liquid water. Therefore, we investigated the corresponding trends in cloud liquid water path under the cloudy conditions, as shown in Fig. 5. We can clearly see that over these areas where such disconnect occurs, the cloud liquid water path has increased and clouds are getting optically thicker. It is also interesting to note that the cloud liquid water is increasing over the parts of southern Sweden and Norway, where the precipitation is also increasing. The same feature is also seen in September along the central western Norwegian coast.

3.3. *Perspectives from the surface measurements*

As mentioned in Section 2, SMHI operates a network of surface radiation measurement stations in Sweden (Fig. 6), many of them operating since many decades and all of them measuring SIS. The perspectives from the station measurements are important for two reasons. First, they provide an independent information and, second, they can be used to evaluate the satellite based estimates. The SIS estimates provided in the CLARA-A2 climate data record are therefore compared with these measurements and the results are shown in Fig. 7. It is found that at nearly all station locations, the correlations between the satellite-based monthly estimates and the ground-based measurements exceed 0.95. In the case of Stations 1 and 5, located in the Scandinavian mountains, the correlations are slightly lower, but nonetheless remain higher than 0.8. The mean bias in CLARA-A2 records is below 5 W/m^2 at the majority of the locations, while the root mean squared biases are below 10 W/m^2 at those locations. It is to be noted that not all stations

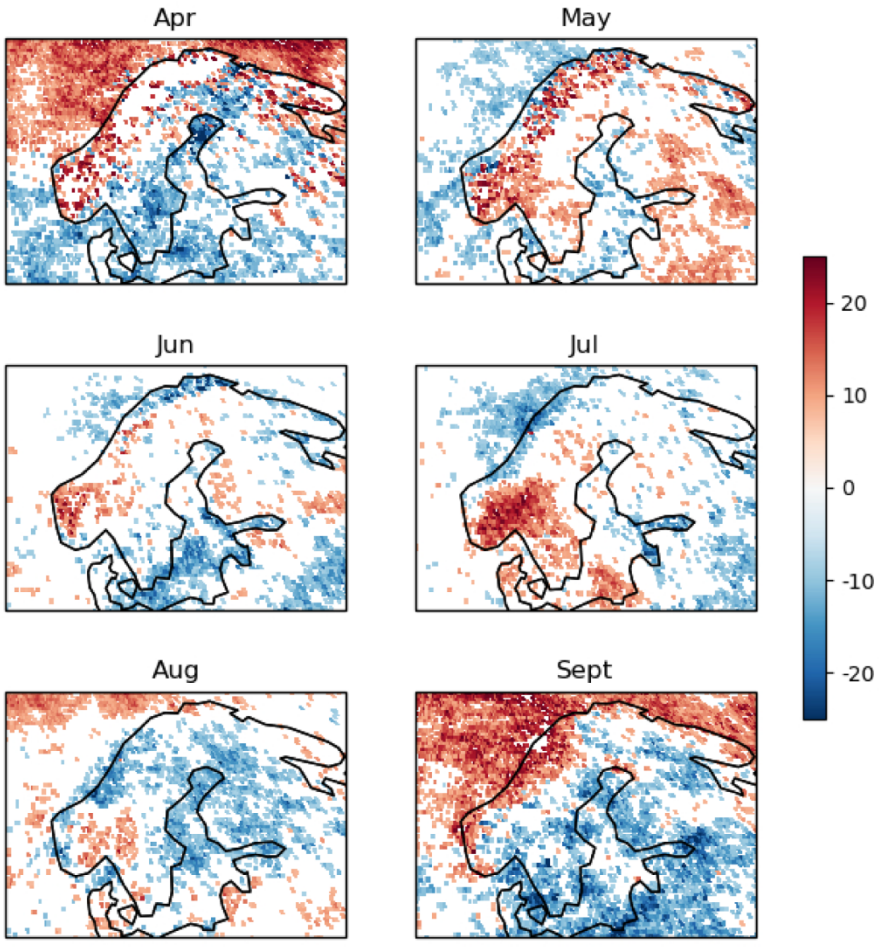

Fig. 5. Trends in cloud liquid water path (g/m^2/decade). Only the trends that are statistically significant at 95% confidence are shown.

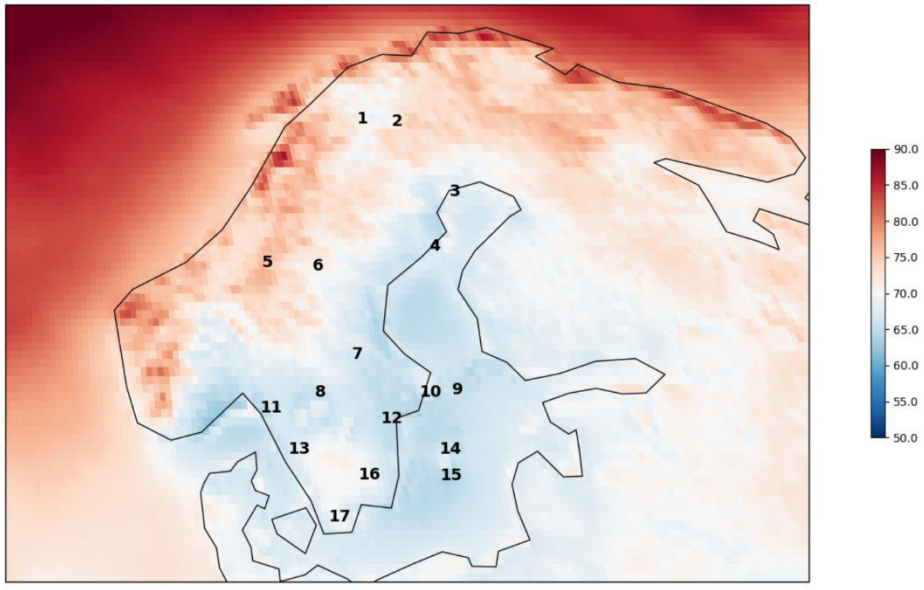

Fig. 6. The locations of 17 surface stations maintained by SMHI, measuring the SIS. The numbers correspond to the Station IDs shown in Table 1. The background shows the 37-year climatological cloud fraction.

have a multidecadal data record available. There are 12 stations that have at least 30 years of data available. These are the stations numbers 2, 3, 4, 6, 7, 8, 10, 12, 13, 16, and 17. Fig. 8 shows the comparison of trends at these 12 locations. It is found that the CLARA-A2 SIS estimates are in excellent agreement with the surface measurements and the sign and magnitude of the trends at all 12 locations agree very well. All 12

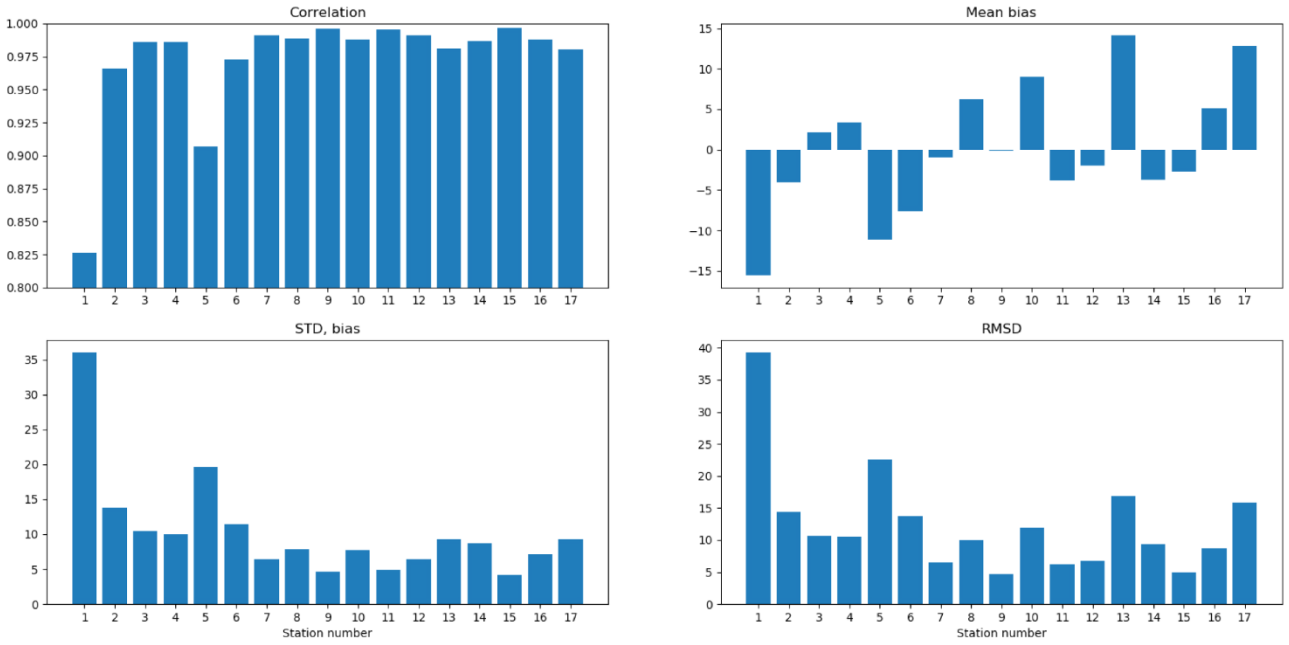

Fig. 7. Comparison of CLARA-A2 SIS with the station measurements. (a) Correlation, (b) Mean bias in W/m^2, (c) Standard deviation of bias in W/m^2 and (d) Root mean squared bias in W/m^2. The X-Axis indicates the station numbers shown in Fig. 6. The data for the AMJJAS months are used to compute the statistics.

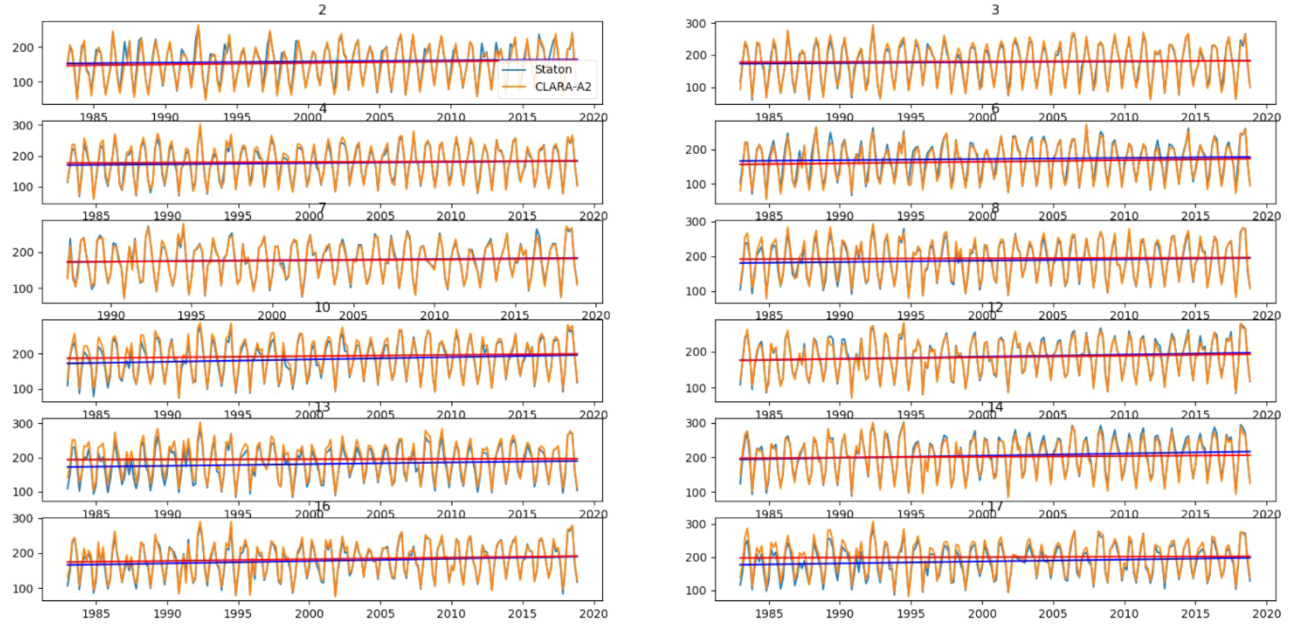

Fig. 8. Comparison of SIS between CLARA-A2 and the surface measurements at the 12 chosen stations. The data for the AMJJAS months from 1983 to 2018 are used.

stations and CLARA-A2 show increasing trends in SIS. Given the fact that we are comparing the point measurements at the stations with the nearest 0.25° grid values from CLARA-A2, these comparison results are highly encouraging and provide confidence in the CLARA-A2 SIS record.

3.4. A key map of agrometeorological trends

The trends in all three variables investigated here, i.e. clouds (C), precipitation (P) and surface radiation (R), are useful climate indicators for the agricultural and forestry applications. We therefore summarize the co-variability of trends among these variables in a key map as shown in Fig. 9. It highlights the categories that show a certain combination of increasing (↑) and decreasing (↓) trends that might be relevant for a particular application. Only those areas where the trends in all three variables are statistically significant are shown. The first category is named "Drier-Murkier-Darker" (P↓C↑R↓), the second category "Drier-Clearer-Brighter" (P↓C↓R↑), the third category "Drier-Clearer-Darker" (P↓C↓R↓), the fourth category "Wetter-Clearer-Brighter" (P↑C↓R↑), the fifth category "Wetter-Murkier-Darker (P↑C↑R↓) and the last one "Wetter-Murkier-Brighter" (P↑C↑R↑).

Such a key map that shows co-dependence among multiple variables is very useful to highlight the geographical hot-spots susceptible to climate change. We indeed see the dominance of three regimes emerging from this key map. The first dominant regime contains the areas that show decreasing trends in both clouds and precipitation and an increasing trend in SIS ("Drier-Clearer-Brighter" (P↓C↓R↑)). The second

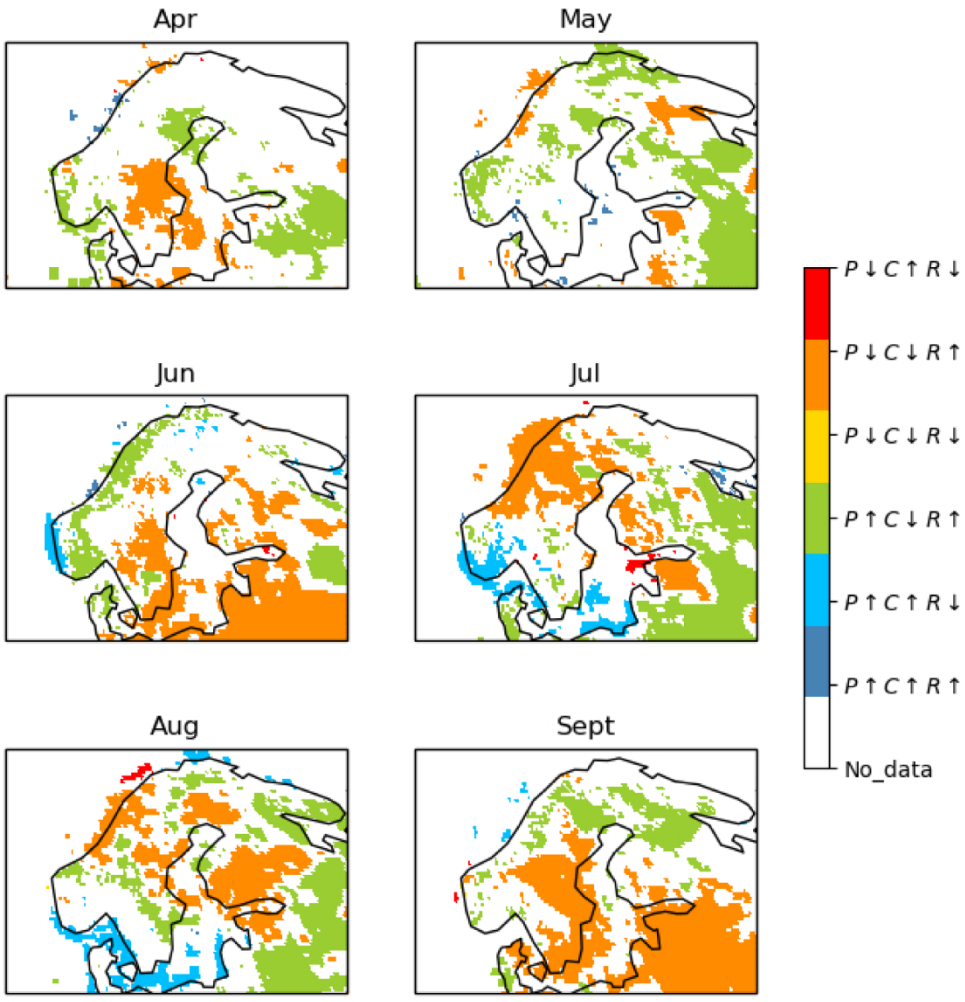

Fig. 9. A key map summarizing the co-variability of trends among cloudiness (C), precipitation (P) and SIS (R). Six different categories are shown with different combinations of trends. The arrows indicate either increasing (↑) or decreasing (↓) trend for each climate variable. These categories are: "Drier-Murkier-Darker" (P↓C↑R↓), "Drier-Clearer-Brighter" (P↓C↓R↑), "Drier-Clearer-Darker" (P↓C↓R↓), "Wetter-Clearer-Brighter" (P↑C↓R↑), "Wetter-Murkier-Darker (P↑C↑R↓) and "Wetter-Murkier-Brighter" (P↑C↑R↑). The co-variability is shown only over those areas where statistically significant trends are observed.

regime contains the areas that show decreasing cloudiness, but increases in both precipitation and SIS ("Wetter-Clearer-Brighter" (P↑C↓R↑)). These are potentially the areas that are likely to benefit most under changing climate in the agrometeorological context. The third regime contain areas that show the increases in both cloudiness and precipitation, but the decreases in SIS ("Wetter-Murkier-Darker" (P↑C↑R↓)). The implications of these regimes are discussed in the next section.

3.5. *Implications for land use and land cover*

The geographical and monthly dependence of the three dominant regimes described in the earlier section is interesting to note in the context of current and future land use and land cover changes relevant to agricultural and forestry practices. In Sweden, according to the most recent estimates from 2018 provided by the EU Copernicus pan-European Land Monitoring Service, 74.73% of land area is covered by the forests, followed by 8.84% by the agricultural areas (https://land.copernicus.eu/pan-european). Due to geographical and climatic conditions, the agricultural areas are predominantly located in the southern Sweden, while the forest cover is densest in the central and northern parts of the country. The global greening trends (Zhu et al., 2016; Dongdong et al., 2017), driven mainly by the CO_2 fertilization, modernization and implementation of better irrigation techniques, improved seed quality, increased agriculture and afforestation in certain regions such as China and India, observed in the last few decades are also to some extent observed over Scandinavia. This greening has however not been homogeneous geographically and seasonally in Scandinavia.

The observed trends in the agrometeorological variables investigated in this study and the resulting interplay among them shown in Section 3.4 could play an important role in either amplifying or dampening the greening trends locally (i.e. changes in the normalized difference vegetation index). For example, in April, the Drier-Clearer-Brighter (P↓C↓R↑) and to some extent Wetter-Clearer-Brighter (P↑C↓R↑) regimes are emerging over the eastern and central parts and as well as in some northern parts of Sweden. The agricultural land use could potentially benefit from these regimes due to increasing radiation and less cloudiness since the agricultural water requirement in this month is minimum as the soil moisture is usually sufficient enough at the beginning of the growing season in spring. Indeed, Dongdong et al. (2017) report a significant greening over these regions in spring. Similarly, in September, increasing trend in surface radiation in the Drier-Clearer-Brighter (P↓C↓R↑) regime over much of the southern, central and eastern Sweden could extend the growing season and benefit agriculture, assuming sufficient water availability in this month. A significant greening in the last few decades is also reported in early autumn over these regions.

In the core summer months of June, July and August, the interplay among the agrometeorology and land use can be even more complex. The intense agricultural activities in these months are highly susceptible to the investigated agrometeorological variables. The Swedish agriculture is about 90% rainfed (Grusson et al., 2021a) and thus heavily dependent on the quantity and regularity of the rainfall during the peak growing season. In June, surface temperatures are warmer and incoming

solar radiation at the surface is intense. At the same time, the water requirement for agriculture and forestry is higher. Given these background conditions, further decreasing precipitation and cloudiness could potentially lead to droughts and have negative impacts on agricultural yields. The fact that the Drier-Clearer-Brighter (P↓C↓R↑) regime is emerging in June over southern Sweden where agriculture is dominant is therefore a cause for concern. The previous studies show that the greening in these peak summer months has indeed been weaker and very heterogenous in the central and southern parts of Sweden (Dongdong et al., 2017). These results show a need for better irrigation services in the future, something that is also argued for when analyzing the current changes in and future climate projections of agricultural changes in Sweden (Grusson et al., 2021b). The length of future agricultural growing seasons is expected to increase in Sweden due to climate change, beginning earlier than normal and also extending well into the late autumn. The vegetation during the peak summer months is however likely to become more negatively susceptible to the changes in agro-meteorological variables and extreme events, if the irrigation and other measures are not adapted to the emerging climate change regimes. Further targeted studies are needed to understand precisely how Scandinavian agriculture would be impacted by changes in agro-meteorological variables in the future (Hoffmann et al, 2021; Grusson et al., 2021b).

4. Conclusions

We investigated recent trends in three agrometeorological/biometeorological climate variables relevant for the agriculture and forestry applications. These are namely, clouds, precipitation and all-sky solar radiation reaching the surface. We used a combination of satellite-based climate data records and ground-based reanalysis and measurements for the 37-year period from 1982 to 2018 for the summer half years (April to September). The results reveal a complex nature of co-variability and trends among these three climate variables over Scandinavia. The following conclusions are drawn from the analysis.

(a) The total cloudiness has decreased over much of Scandinavia. The decrease is most pronounced and statistically significant over southern Scandinavia in April, over the western coast in July and over much of northern Scandinavia in August.

(b) These decreasing trends are mainly due to reductions in the low and middle level clouds, while the high level clouds show statistically significant increases during the late summer months.

(c) The trends in all-sky incoming surface radiation are opposite in nature and broadly follow the spatio-temporal patterns of the trends in total cloudiness.

(d) In contrast to the trends in cloudiness, the precipitation trends are heterogeneous, both spatially and temporally. While most of the precipitation trends can be explained by the corresponding trends in cloudiness, there is certain disconnect between the trends of these two variables. This disconnect can be in part explained by the changes in the opacity or water holding capacity of clouds.

(e) The satellite-based estimates of all-sky surface radiation agree strongly with the surface measurements and show similar increasing trends as well, confirming the validity and robustness of the satellite based records of SIS.

(f) A key agrometeorological map summarizing the co-variability of trends reveals three distinct area-regimes that are relevant for assessing the changes in the agricultural and forestry practices.

The results further provide an observational basis for the evaluation of Earth System Models that have a vegetation component. For example, it could be examined if these models show similar trends among the climate variables studied here and if their co-variability also reveals similar area-regimes. This will help in the assessment of the projected changes in the land use and land cover in future scenarios, especially those relevant for agricultural and forestry applications.

Declaration of Competing Interest

The authors declare that they have no known competing financial interests or personal relationships that could have appeared to influence the work reported in this paper.

References

Ambros, P., Granvik, M., 2020. Trends in Agricultural land in EU countries of the Baltic Sea region from the perspective of resilience and food security. Sustainability 12 (14), 5851. https://doi.org/10.3390/su12145851.

Becker, A., Finger, P., Meyer-Christoffer, A., Rudolf, B., Schamm, K., Schneider, U., Ziese, M., 2013. A description of the global land-surface precipitation data products of the global precipitation climatology centre with sample applications including centennial (trend) analysis from 1901–present. Earth Syst. Sci. Data. https://doi.org/10.5194/essd-5-71-2013.

Carlund, T., 2011. Upgrade of SMHI's meteorological radiation network 2006–2007. SMHI Meteorol. Available online https://www.smhi.se/publikationer/upgrade-of-smhi-s-meteorological-radiation-network-2006-2007-effects-on-direct-and-global-solar-radiation-1.19033 (accessed on 30 March 2021).

Carlund, T., 2013. Baltic region pyrheliometer comparison 2012: 21 May 2012–1 June 2012, Norrköping, Sweden. WMO, Geneva, Switzerland. Instruments and Observing Methods Report No. 112Available online. https://www.wmo.int/pages/prog/www/IMOP/publications-IOM-series.html (accessed on 30 March 2021).

Cheng, S.J., Steiner, A.L., Hollinger, D.Y., Bohrer, G., Nadelhoffer, K.J., 2016. Using satellite-derived optical thickness to assess the influence of clouds on terrestrial carbon uptake. J. Geophys. Res. Biogeosci. 121, 1747–1761. https://doi.org/10.1002/2016JG003365.

Chmielewski, F.M., Rötzer, T., 2001. Response of tree phenology to climate change across Europe. Agric. For. Meteorol. 108 (2), 101–112. https://doi.org/10.1016/S0168-1923(01)00233-7, 2001ISSN 0168-1923.

Devasthale, A., Norin, L., 2014. The large-scale spatio-temporal variability of precipitation over Sweden observed from the weather radar network. Atmos. Meas. Tech. 7, 1605–1617. https://doi.org/10.5194/amt-7-1605-2014.

Dybbroe, A., Karlsson, K., Thoss, A., 2005. NWCSAF AVHRR cloud detection and analysis using dynamic thresholds and radiative transfer modeling. Part I: algorithm description. J. Appl. Meteorol. 44 (1), 39–54.

Gu, L., Fuentes, J.D., Shugart, H.H., Staebler, R.M., Black, T.A., 1999. Responses of net ecosystem exchanges of carbon dioxide to changes in cloudiness: results from two North American deciduous forests. J. Geophys. Res. 104 (D24), 31421–31434. https://doi.org/10.1029/1999JD901068.

Guenni, L., Rose, C.W., Hogarth, W., Braddock, R.D., Charles-Edwards, D., 1990. Seasonal changes in interrelationships between climatic variables. Agric. For. Meteorol. 53 (1–2), 45–58. https://doi.org/10.1016/0168-1923(90)90123-N, 1990ISSN 0168-1923.

Gulev, S.K., Thorne, P.W., Ahn, J., Dentener, F.J., Domingues, C.M., Gerland, S., Gong, D., Kaufman, D.S., Nnamchi, H.C., Quaas, J., Rivera, J.A., Sathyendranath, S., Smith, S.L., Trewin, B., von Schuckmann, K., Vose, R.S., MassonDelmotte, V., Zhai, P., Pirani, A., Connors, S.L., Péan, C., Berger, S., Caud, N., Chen, Y., Goldfarb, L., Gomis, M.I., Huang, M., Leitzell, K., Lonnoy, E., Matthews, J.B.R., Maycock, T.K., Waterfield, T., Yelekçi, O., Yu, R., Zhou, B., 2021. 2021: changing state of the climate system. Climate Change 2021: The Physical Science Basis. Contribution of Working Group I to the Sixth Assessment Report of the Intergovernmental Panel on Climate Change. Cambridge University Press (eds.)In Press.

Grusson, Y., Wesström, I., Joel, A., 2021a. Impact of climate change on Swedish agriculture: growing season rain deficit and irrigation need. Agric. Water Manag. 251, 106858 https://doi.org/10.1016/j.agwat.2021.106858.

Grusson, Y., Wesström, I., Svedberg, E., Joel, A., 2021b. Influence of climate change on water partitioning in agricultural watersheds: examples from Sweden. Agric. Water Manag. 249, 106766 https://doi.org/10.1016/j.agwat.2021.106766. ISSN 0378-3774.

Hoffmann, P., Reinhart, V., Rechid, D., de Noblet-Ducoudré, N., Davin, E.L., Asmus, C., Bechtel, B., Böhner, J., Katragkou, E., Luyssaert, S., 2021. High-resolution land-use land-cover change data for regional climate modelling applications over Europe – part 2: historical and future changes. Earth Syst. Sci. Data Discuss. https://doi.org/10.5194/essd-2021-252 [preprint]in review.

[Core Writing Team IPCC, Pachauri, R.K., Meyer, L.A., 2014. Climate change 2014: synthesis report. Contribution of Working Groups I, II and III to the Fifth Assessment Report of the Intergovernmental Panel on Climate Change. IPCC, Geneva, Switzerland, p. 151 [Core Writing Team(eds.)]pp.

Jia, G., Shevliakova, E., Artaxo, P., De Noblet-Ducoudré, N., Houghton, R., House, J., Kitajima, K., Lennard, C., Popp, A., Sirin, A., Sukumar, R., Verchot, L., Shukla, P.R., Skea, J., Calvo Buendia, E., Masson-Delmotte, V., Pörtner, H.O., Roberts, D.C., Zhai, P., Slade, R., Connors, S., Van Diemen, R., Ferrat, M., Haughey, E., Luz, S., Neogi, S., Pathak, M., Petzold, J., Portugal Pereira, J., Vyas, P., Huntley, E., Kissick, K., Belkacemi, M., Malley, J., 2019. Land–climate interactions. Climate Change and Land: An Special Report on Climate Change, Desertification, Land Degradation, Sustainable Land Management, Food Security, and Greenhouse Gas Fluxes in Terrestrial Ecosystems. IPCC (eds.)In press.

Jin, H., Jönsson, A.M., Olsson, C., et al., 2019. New satellite-based estimates show significant trends in spring phenology and complex sensitivities to temperature and precipitation at northern European latitudes. Int. J. Biometeorol. 63, 763–775. https://doi.org/10.1007/s00484-019-01690-5.

Jönsson, A.M., Lagergren, F., 2017. Potential use of seasonal forecasts for operational planning of north European forest management. Agric. For. Meteorol. 244–245, 122–135. https://doi.org/10.1016/j.agrformet.2017.06.001. ISSN 0168-1923.

Kanniah, K.D., Beringer, J., Hutley, L., 2013. Exploring the link between clouds, radiation, and canopy productivity of tropical savannas. Agric. For. Meteorol. 182–183, 304–313. https://doi.org/10.1016/j.agrformet.2013.06.010, 2013ISSN 0168-1923.

Karlsson, K.G., 2003. A 10 year cloud climatology over Scandinavia derived from NOAA Advanced very high resolution radiometer imagery. Int. J. Climatol. 23, 1023–1044. https://doi.org/10.1002/joc.916.

Karlsson, K.G., Dybbroe, A., 2010. Evaluation of Arctic cloud products from the EUMETSAT climate monitoring satellite application facility based on CALIPSO-CALIOP observations. Atmos. Chem. Phys. 10, 1789–1807. https://doi.org/10.5194/acp-10-1789-2010.

Karlsson, K.G., Riihelä, A., Müller, R., Meirink, J.F., Sedlar, J., Stengel, M., Lockhoff, M., Trentmann, J., Kaspar, F., Hollmann, R., Wolters, E., 2013. CLARA-A1: a cloud, albedo, and radiation dataset from 28yr of global AVHRR data. Atmos. Chem. Phys. 13, 5351–5367. https://doi.org/10.5194/acp-13-5351-2013.

Karlsson, K.G., Anttila, K., Trentmann, J., Stengel, M., Meirink, F., et al., 2017. CLARA-A2: the second edition of the CM SAF cloud and radiation data record from 34 years of global AVHRR data. Atmos. Chem. Phys. 17, 5809–5828. https://doi.org/10.5194/acp-17-5809-2017.

Karlsson, K.G., Devasthale, A., 2018. Inter-Comparison and evaluation of the four longest satellite-derived cloud climate data records: CLARA-A2, ESA cloud CCI V3, ISCCP-HGM, and PATMOS-x. Remote Sens. 10 (10), 1567. https://doi.org/10.3390/rs10101567.

Kendall, M.G., 1975. Rank Correlation Methods, 4th ed. Charles Griffin, London, p. 202. pp.

Keskitalo, E.C., Bergh, J., Felton, A., Björkman, C., Berlin, M., et al., 2016. Adaptation to climate change in Swedish forestry. Forests 7 (2), 28. https://doi.org/10.3390/f7020028.

Kjellström, E., Nikulin, G., Strandberg, G., Christensen, O.B., Jacob, D., Keuler, K., Lenderink, G., van Meijgaard, E., Schär, C., Somot, S., Sørland, S.L., Teichmann, C., Vautard, R., 2018. European climate change at global mean temperature increases of 1.5 and 2 °C above pre-industrial conditions as simulated by the EURO-CORDEX regional climate models. Earth Syst. Dyn. 9, 459–478. https://doi.org/10.5194/esd-9-459-2018.

Dongdong, K., Zhang, Q., Singh, V.P., Shi, P., 2017. Seasonal vegetation response to climate change in the Northern Hemisphere (1982–2013). Glob. Planet. Change 148, 1–8. https://doi.org/10.1016/j.gloplacha.2016.10.020. ISSN 0921-8181.

Krauskopf, T., Huth, R., 2020. Temperature trends in Europe: comparison of different data sources. Theor. Appl. Climatol. 139, 1305–1316. https://doi.org/10.1007/s00704-019-03038-w.

Lagergren, F., Lindroth, A., 2002. Transpiration response to soil moisture in pine and spruce trees in Sweden. Agric. For. Meteorol. 112 (2), 67–85. https://doi.org/10.1016/S0168-1923(02)00060-6. ISSN 0168-1923.

Mann, H.B., 1945. Nonparametric tests against trend. Econometrica 13, 245–259. https://doi.org/10.2307/1907187.

Norin, L., Devasthale, A., L'Ecuyer, T.S, 2017. The sensitivity of snowfall to weather states over Sweden. Atmos. Meas. Tech. 10, 3249–3263. https://doi.org/10.5194/amt-10-3249-2017.

Pfeifroth, U., Sanchez-Lorenzo, A., Manara, V., Trentmann, J., Hollmann, R., 2018. Trends and variability of surface solar radiation in Europe based on surface- and satellite-based data records. J. Geophys. Res. Atmos. 123, 1735–1754. https://doi.org/10.1002/2017JD027418.

Proctor, J., 2021. Atmospheric opacity has a nonlinear effect on global crop yields. Nat. Food 2, 166–173. https://doi.org/10.1038/s43016-021-00240-w.

Riihelä, A., Carlund, T., Trentmann, J., Müller, R., Lindfors, A.V., 2015. Validation of CM SAF surface solar radiation datasets over Finland and Sweden. Remote Sens. 7, 6663–6682. https://doi.org/10.3390/rs70606663.

Rutgersson, A., et al., 2015. Recent change—atmosphere. The BACC II Author Team Second Assessment of Climate Change for the Baltic Sea Basin. Regional Climate Studies Springer, Cham. https://doi.org/10.1007/978-3-319-16006-1_4.

Schneider, U., Becker, A., Finger, P., Meyer-Christoffer, A., Ziese, M., Rudolf, B., 2014. GPCC's new land surface precipitation climatology based on quality-controlled *in situ* data and its role in quantifying the global water cycle. Theor. Appl. Climatol. 115, 15–40. https://doi.org/10.1007/s00704-013-0860-x.

Schurgers, G., Lagergren, F., Mölder, M., Lindroth, A., 2015. The importance of micrometeorological variations for photosynthesis and transpiration in a boreal coniferous forest. Biogeosciences 12, 237–256. https://doi.org/10.5194/bg-12-237-2015.

Sikma, M., Ouwersloot, H.G., Pedruzo-Bagazgoitia, X., van Heerwaarden, C.C, Vilà-Guerau de Arellano, J., 2018. Interactions between vegetation, atmospheric turbulence and clouds under a wide range of background wind conditions. Agric. For. Meteorol. 255, 31–43. https://doi.org/10.1016/j.agrformet.2017.07.001, 2018ISSN 0168-1923.

Skogsstyrelsen, 2019. Klimatanpassning av skogen och skogsbruket – mål och förslag på åtgärder, Rapport 2019/23, pp 1–67. https://www.skogsstyrelsen.se/globalassets/om-oss/rapporter/rapporter-2021202020192018/rapport-2019-23-klimatanpassning-av-skogen-och-skogsbruket.pdf.

Still, C.J., et al., 2009. Influence of clouds and diffuse radiation on ecosystem-atmosphere CO_2 and $CO^{18}O$ exchanges. J. Geophys. Res. 114 https://doi.org/10.1029/2007JG000675. G01018.

Young, D.R., Smith, W.K., 1983. Effect of Cloudcover on photosynthesis and transpiration in the subalpine understory species arnica latifolia. Ecology 64 (4), 681–687. https://doi.org/10.2307/1937189.

Wang, S., Zhang, Y., Ju, W., Chen, J.M., Ciais, P., Cescatti, A., Sardans, J., Janssens, I.A., Wu, M., Berry, J.A., Campbell, E., Fernández-Martínez, M., Alkama, R., Sitch, S., Friedlingstein, P., Smith, W.K., Yuan, W., He, W., Lombardozzi, D., Kautz, M., Zhu, D., Lienert, S., Kato, E., Poulter, B., Sanders, T.G.M., Krüger, I., Wang, R., Zeng, N., Tian, H., Vuichard, N., Jain, A.K., Wiltshire, A., Haverd, V., Goll, D.S., Peñuelas, J., 2020. Recent global decline of CO_2 fertilization effects on vegetation photosynthesis. Science 370 (6522), 1295–1300. https://doi.org/10.1126/science.abb7772, 2020 Dec 11Erratum in: Science. 2021 Feb 5;371(6529): PMID: 33303610.

Watson, J., Challinor, A.J., 2013. The relative importance of rainfall, temperature and yield data for a reginal-scale crop model. Agric. For. Meteorol. 170, 47–57 pp.

Zhu, Z., Piao, S., Myneni, R., et al., 2016. Greening of the earth and its drivers. Nat. Clim. Change 6, 791–795. https://doi.org/10.1038/nclimate3004.